



The adult plant resistance (APR) genes *Yr18*, *Yr29* and *Yr46* in spring wheat showed significant effect against important yellow rust races under North-West European field conditions

Ondřej Zelba · Sarah Wilderspin · Amelia Hubbard · Charlotte F. Nellist · Anders Krogh Mortensen · Philipp Schulz · Julio Huerta-Espino · Ravi Singh · Chris Khadgi Sørensen

Received: 9 January 2024 / Accepted: 21 May 2024 / Published online: 17 June 2024
© The Author(s) 2024

Abstract Yellow rust caused by *Puccinia striiformis* f. sp. *tritici* (*Pst*) is one of the most important wheat diseases. Adult plant resistance (APR) genes have gained the attention of breeders and scientists because they show higher durability compared to major race-specific genes. Here, we determined the effect of the APR genes *Yr18*, *Yr29* and *Yr46* in North-West European field conditions against three currently important *Pst* races. We used three pairs of sibling wheat lines developed at CIMMYT, which

consisted of a line with the functional resistance gene and a sibling with its non-functional allele. All APR genes showed significant effects against the *Pst* races Warrior and Warrior (–), and a race of the highly aggressive strain *PstS2*. The effects of *Yr18* and *Yr46* were especially substantial in slowing down disease progress. This effect was apparent in both Denmark, where susceptible controls reached 100 percent disease severity, and in United Kingdom where disease pressure was lower. We further validated field results by quantifying fungal biomass in leaf samples and by micro-phenotyping of samples collected during early disease development. Microscopic image analyses

Supplementary Information The online version contains supplementary material available at <https://doi.org/10.1007/s10681-024-03355-w>.

O. Zelba
Department of Genetics and Plant Breeding Methods, Crop Research Institute, Drnovská 507, Ruzyně, 161 06 Prague, Czech Republic

O. Zelba
Faculty of Tropical AgriSciences, Czech University of Life Sciences, Prague, Czech Republic

S. Wilderspin · A. Hubbard · C. F. Nellist
Cambridge Crop Research, NIAB, Cambridge, UK

A. K. Mortensen
Department of Electrical and Computer Engineering, Aarhus University, 8200 Aarhus, Denmark

P. Schulz
Federal Research Centre for Cultivated Plants, Julius Kühn-Institut, Institute for Plant Protection in Field Crops and Grassland, Kleinmachnow, Germany

J. Huerta-Espino
Campo Experimental Valle de México INIFAP, Apdo. Postal 10, 56230 Chapingo, Mexico

R. Singh
International Maize and Wheat Improvement Center (CIMMYT), Texcoco, Mexico

R. Singh
Huazhong Agricultural University, Wuhan 430070, China

C. K. Sørensen (✉)
Department of Agroecology, Aarhus University, 4200 Slagelse, Denmark
e-mail: chris.sorensen@agro.au.dk

using deep learning allowed us to quantify separately the APR effects on leaf colonization and pustule formation. Our results show that the three APR genes can be used in breeding yellow rust resistant varieties of spring wheat to be grown in North-West European conditions, and that deep learning image analysis can be an effective method to quantify effects of APR on colonisation and pustule formation.

Keywords Spring wheat · Resistance breeding · Phenotyping · *Puccinia striiformis* · Micro-phenotyping · Deep learning

Introduction

Cereal rusts are among the most significant constraints on wheat production worldwide. Stem rust, yellow rust, and leaf rust are caused by biotrophic fungal pathogens from the genus *Puccinia*. The fungal pathogens are characterized by infecting and colonizing the cereal host and subsequently producing pustules on the plant surface. Pustules produce masses of spores that are released to the environment, able to infect the cereal host. This may result in cycles of reinfections that can lead to epidemics. The spores are also capable of a long-distance dispersal, allowing the disease to spread over large areas every growing season. When rust diseases are not regulated, the severely infested field's yields are reduced (Roelfs et al. 1992).

Yellow (or Stripe) rust of wheat is caused by *P. striiformis* f. sp. *tritici* (*Pst*). This pathogen's worldwide populations have undergone significant changes during recent past. An adaptation to warmer climate and a higher aggressiveness can be seen in the closely related strains *Pst*S1/S2 that have caused severe epidemics since 2000 in e.g., United States, East Africa, and Australia (Hovmøller et al. 2008; Milus et al. 2009). Such changes in the pathogen's biology increased the geographical reach and the ability to cause more substantial economic losses (Beddow et al. 2015). In the case of Europe, incursions of genetic groups *Pst*S7 with the Warrior race and *Pst*S8 with the Kranich race replaced the previous populations after 2011 (Ali et al. 2017). These races probably emerged from the Himalayan region by sexual recombination on the alternate host (Hovmøller et al. 2016). Currently the European *Pst* landscape is

dominated by the *Pst*S10 genetic group including the typical Warrior (–) race (Ali et al. 2017).

The most sensible protection from rusts is to grow resistant cultivars. The resistance genes that are present in such cultivars can be categorized based on several criteria (Wang and Chen 2017). Most commonly a distinction is made between all-stage resistance and adult plant resistance (APR) based on the growth stage during which the resistance is effective. All-stage resistance is based on single race-specific genes (R-genes), most often with major qualitative effects, whereas APR is quantitatively inherited and often polygenic. Another important factor of resistance is the race-specificity—some resistance genes are race-specific while others are seemingly effective against all known races of the pathogen (Ellis et al. 2014). APR is usually considered non-race-specific and more durable, but this is not a general rule, as it was demonstrated on APR quantitative trait loci (QTLs) that lost their efficacy against novel *Pst* races in Europe (Sørensen et al. 2014). Individual APR genes provide only partial resistance but often with additive effects. APR is influenced by environmental factors and effects can be difficult to measure accurately. Therefore, breeding lines are usually tested in different locations for evaluation of APR effects, such as in the case of the International Maize and Wheat Improvement Center (CIMMYT) breeding program (Singh et al. 2011). By combining APR genes with additive effects in the same cultivar it is possible to achieve high resistance levels that are stable across environments (Singh et al. 2011).

As combining APR genes is important to achieve durable resistance in the field, this category attracts considerable attention from scientists and breeders. Three of the most studied genes *Yr*18, *Yr*29, and *Yr*46 are pleiotropic and effective against multiple pathogens including all three wheat rusts and powdery mildew (*Blumeria graminis* f. sp. *tritici*). Their more complete designations are *Lr*34/*Yr*18/*Sr*57/*Pm*38, *Lr*46/*Yr*29/*Sr*58/*Pm*39, and *Lr*67/*Yr*46/*Sr*55/*Pm*46, respectively. A leaf-tip necrosis is a typical phenotypic trait that can be observed in lines harbouring these genes. *Yr*18 was successfully cloned and was shown to encode an adenosine-triphosphate binding cassette (ABC) transporter (Krattinger et al. 2009). It is present in world wheat germplasm in the form of distinct alleles in both spring and winter wheats; however, it is most common in cultivars developed at

CIMMYT where it descended from ‘Mentana’ and subsequently ‘Frontana’ wheats (Kolmer et al. 2008). *Yr46* encodes a sugar-transporter protein (STP) and is present in historical CIMMYT germplasm. Its resistance allele seems to have disappeared from wheat breeding along with the effort to produce semi-dwarf varieties during the Green Revolution (Moore et al. 2015). *Yr29*, first identified on chromosome 1B in the cultivar Pavon 76 (Singh et al. 1998), is yet to be cloned but preliminary studies suggest a different mechanism than *Yr18* (Lagudah 2011). The understanding of molecular mechanisms behind these APR genes suggests that they are fundamentally different to major R-genes and that they also differ from each other.

At times of rapid and worldwide rust population shifts, this study aims to further expand the knowledge about pleiotropic APR genes and their ability to provide a general defence in wheat under different environmental conditions, against yellow rust strains of economic importance. In inoculated field trials in Denmark and the United Kingdom (UK), we tested the effect of the APR genes *Yr18*, *Yr29* and *Yr46* in spring wheat against races of the important *Pst* genetic groups *PstS2*, *PstS7* and *PstS10*.

Materials and methods

Wheat lines and pathogen isolates

Three pairs of spring wheat sibling lines from CIMMYT were selected for field trials (Table 1). Each pair comprises a line with a functional APR gene and a susceptible sibling control line. The APR genes under investigation were *Yr18*, *Yr29*, and *Yr46*. Additionally, cv. Avocet S was included as a control susceptible to all pathogen isolates used and cv. Morocco was used as a disease spreader. Field trials were carried out at research centre Flakkebjerg, Aarhus University (AU), Denmark (N 55° 19' 30 E 11° 23' 25) and at NIAB, Cambridge, UK (N 52° 15' 41.8 E 0° 01' 13.3) during the 2021 season.

To avoid the masking effect of any potential all-stage resistance genes, the wheat lines were initially tested in the greenhouse against *Pst* isolates representing the genetic groups *PstS0–PstS14* (Hovmøller et al. 2023). Inoculation and assessment were done according to Hovmøller et al. (2017) and results given in Supplementary File 1. Based on this, *Pst* isolates DK46/14 and DK66/02 were selected to be used in the Danish field trials and isolates UK16/035 and UK19/215 were selected for the UK field trials. DK46/14 and UK16/035 represent the Warrior (–) race and belong to the genetic group *PstS10*. DK66/02 represents the genetic group *PstS2*, and Isolate UK19/215 represents the Warrior race and belongs to genetic group *PstS7*. Pathogen inoculum

Table 1 Description of plant materials used in experiments

Line designation used in this study	Cross or variety name	Resistance genes	Original source ^a
<i>Yr18</i>	LALB (PRL7D)	<i>Lr34/Yr18</i> -Resistant sib	CIMMYT ^b
Control (<i>Yr18</i>)	LALB (PRL7D)	<i>Lr34/Yr18</i> -Susceptible mutant	CIMMYT ^b
<i>Yr29</i>	LALBMONO1*4/PVN	<i>Lr46/Yr29</i> -Resistant sib	CIMMYT ^b
Control (<i>Yr29</i>)	LALBMONO1*4/PVN	<i>Lr46/Yr29</i> -Susceptible mutant	CIMMYT ^b
<i>Yr46</i>	RL6077/AOC-YR	<i>Lr67/Yr46</i> -Resistant sib	CIMMYT ^b
Control (<i>Yr46</i>)	RL6077/AOC-YR	<i>Lr67/Yr46</i> -Susceptible mutant (15 bp deletion)	CIMMYT ^b
Avocet.S	Avocet.S	Susceptible control: Susceptible to <i>PstS2</i> and Warrior (–) races	Wellings ^c
Disease spreader	Morocco	Susceptible variety (disease spreader)	ICARDA ^d

^aAll seeds were multiplied at the Global Rust Reference Center, AU, Denmark before experiments

^bInternational maize and wheat improvement center

^cWellings et al. (2009)

^dInternational center for agricultural research in the dry areas

was produced in the greenhouse. For the AU trials, seedlings of susceptible cv. Morocco were grown in 7×7 cm pots (15–20 plants per pot) and inoculated after emergence of second leaf using the airbrush method (Sørensen et al. 2016). After inoculation, the plants were incubated at 10 °C for 24 h and transferred to spore-proof greenhouse cabins until the sporulation was sufficient and the plants were ready to be used. Inoculum for different genotypes was always kept separately. For the UK trials, seedlings of the susceptible cv. Warrior (for UK16/035) and KWS Extase (for UK19/215) were grown in 51×33 cm multi-trays containing 35 cells per tray (15 plants per cell), and the plants were inoculated after emergence of the second leaf with urediniospores suspended in talcum powder at the spore:talcum powder ratio of 1:16. The inoculum was applied to leaves using compressed air and a spinning platform. After inoculation plants were incubated in the dark at 8 °C for 48 h and transferred to spore-proof growth chambers with a temperature regime of 18 °C day, 11 °C night with a 16 h daylength until sporulation was sufficient. Inoculum for different genotypes were kept separately.

Experimental design and field assessments

Field trials at AU and NIAB followed the same experimental design. The wheat lines were sown at the end of March 2021 in one square meter plots, each consisting of six rows. In each plot, two rows were one test line, two rows a second test line, and in between test lines were two spreader rows of cv. Morocco. The total plots were distributed according to a randomised complete block design with three replicates. Trials for different rust races were sown at separate locations, repeating the same block design on the two locations. Spreader rows were inoculated at tillering stage on a day with suitable weather conditions using the previously prepared diseased plants from the greenhouse. The diseased plants with spores were gently swept across all plants in the spreader rows in one direction, and this process was repeated on the next day in the opposite direction to ensure sufficient infection. Plots were closely monitored, and disease assessments started shortly after first symptoms began to appear. Disease severity was assessed four times during the growing season seven-eight days apart using the modified Cobb Scale (Peterson et al. 1948). In the UK trials, disease assessments were done at growth stage

47, 55, 60 and 65/69 and in the AU trials, plants were assessed at growth stage 59, 65, 73, and 80 according to Zadoks et al. (1974). The upper three leaves were rated for all plants in a row and an estimate average was recorded for each replicate. In the AU trials, all spikes of the tested lines were harvested at maturity and bulk threshed. Thousand-grain weight (TGW) was estimated by weighing a thousand randomly chosen kernels per replicate. TGW was similarly measured for greenhouse-grown and disease-free control plants of all lines.

Fungal biomass quantification

The flag leaves for fungal biomass quantification were collected in the AU trial on the first date of disease scoring and again 15 days later. Sampling was not done at the latest scoring date because the leaves were too senescent and clearly secondary fungal infections had started to appear. On each date, five whole flag leaves were sampled per treatment from each of the three biological replicates. Fungal biomass in infected leaves was quantified by staining fungal chitin in the infected leaves with fluorescein conjugated wheat germ agglutinin (WGA-FITC) according to Ayliffe et al. (2013). Each sample was weighted in the laboratory and stored submerged in 1M KOH in 50 mL falcon tubes until further procedure. After discarding KOH, the tissue was submerged in five times its weight of 0.05 M Tris-HCl (pH 7.0). The tissue was homogenized using a laboratory tissue homogenizer (IKA-Werke GmbH & Co. KG, Staufen, Germany). Three individual 100 µL repetitions of each sample were stained in PCR strips or plates with 5 µL WGA-FITC (1 mg/mL) (Sigma-Aldrich, St. Louis, MO, USA) for 1 h at room temperature (RT). Samples were then washed three times in 0.05M Tris-HCl (pH 7.0) before measuring fluorescence using a Biotek Synergy 2 microplate reader (BioTek Instruments, Inc., Winooski, VT, USA) in a suitable microplate. The settings were 485 nm for excitation and 530 nm for emission, the reads were repeated three times.

Microscopy and image analysis

Three flag leaves were sampled per replicate (in total 9 leaves per wheat line) in the *PstS2* field trial at AU on the same date as the first disease severity assessment. It was done to compare the effect of the

individual APR genes on fungal growth and to estimate the match between early disease establishment in the leaves and the final disease level. Only a few pustules were visible on the flag leaf at sampling. Fungal colonies in the leaves were stained according to the WGA-FITC method (Ayliffe et al. 2013) with a few modifications. In brief, leaves were submerged in 1M KOH in 50 mL falcon tubes and heated to 80 °C for 30 min in a water bath. The KOH solution was poured off and replaced with 50 mM Tris-HCl (pH 7.5) to neutralize the samples. Samples were shaken for 20 min and the neutralisation step was repeated three times. Finally, fresh Tris-HCl buffer was added to cover the leaves, and 10 µL of WGA-FITC (Sigma-Aldrich, St. Louis, MO, USA) per mL buffer was added from a working solution of 1 mg/mL. Samples were left in the refrigerator at 5 °C until observation under the microscopy. Leaf samples were mounted on glass slides in 50% (w/w) glycerol with a cover glass and viewed under a Zeiss Axioplan 2 microscope equipped with a Colibri 7 LED light source (Zeiss). Samples were observed at 5× magnification using 475 nm LED light and filter set 90 HE LED (Zeiss). Forty-eight images in a 12×4 matrix with 10% overlap were recorded per leaf parallel to the leaf veins. Image acquisition was done in approximately the same central part on all leaf samples to ensure unbiased sampling. All images were captured with an Axiocam 705 colour camera (Zeiss). The 48 images per leaf were stitched together using the grid/collection stitching plugin in Fiji (ImageJ) (Schindelin et al. 2012). The stitched image covered a leaf area of approximately 2.9×1 cm (Length×width). For further analysis, the stitched images were converted to 8-bit format. Since only fungal tissue was stained and emitted fluorescent light in the images, a simple threshold function in Fiji was used to quantify the amount. Any pixels in the value range of 25–255 were assumed to show fungal tissue and subsequently the histogram function was used to extract the leaf area under infection.

To quantify the area of uredinia in the stitched images, first a training set of 150 images containing uredinia was created from the dataset, with a uniform size of 1024×1024 pixels (px). For this training set, a corresponding set of masks covering the uredinia (area with visible sporulation) was created by hand. This training set was used to train a convolutional neural network (CNN) model with U-Net architecture

(Falk et al. 2018) via the ZeroCostDL4Mic platform (von Chamier et al. 2021). Advanced settings for training were left to default (batch size=4, patch size=512×512 px, pooling steps=2, and 10% of patches used for validation) and no image augmentation was used to enhance the training set. After training, the model was tested on an unseen set of 12 images and model predictions were compared to human-made masks. The final model was then used for segmentation of the whole microscopy dataset using ZeroCostDL4Mic platform. Only images containing at least 1% of fungal tissue were processed, as the model showed false results when there was no fungal tissue present at all. Predictions generated by the model were saved and processed in Fiji using the threshold function set for range 245–255. Background noise in the predictions was cleaned up using MorphoLibJ (Legland et al. 2016) filters with the same settings for all images. The accuracy of the predictions was visually checked after each step. The ratio of area with sporulation against total leaf area was then extracted from each image using the histogram function. Evaluation of the model training including training and validation loss plots can be seen in Supplementary File 2. The model was published online (<https://zenodo.org/doi/10.5281/zenodo.8260661>) for further use or re-training.

Statistical methods

Means of disease severity evaluations from the four different time points were used to calculate area under disease progress curve (AUDPC) (Wilcoxon et al. 1975). For biomass and the image-based parameters, a mean was calculated across technical replicates or repeated leaf measurements within replicates, respectively, and used as experimental unit in the statistical analysis. Statistical comparison between the resistant and the susceptible line in each sibling pair were for all parameters done by *t*-tests using the *t*-test function in R (R Core Team 2021). Before comparisons, tests for equal variance were done using the var. test function. In case of equal variance students *t*-tests were performed, otherwise Welch's *t*-tests were used. Tests for normal distribution in each data set as a prerequisite for performing a parametrical *t*-test were done by Q-Q (quantile–quantile) plots of standardized residuals resulting from a one-way ANOVA (analysis of variance) in R. One-way ANOVA was

done individually for each race using wheat line as the only factor since pathogen race factor levels were not crossed in the experimental design. All graphs in the article were plotted in R Studio using the `ggplot2` package (Wickham 2009).

Results

Disease progress in the field

Transfer of disease via the spreader row into the experimental plots was successful in all trials although disease progression was slower in the NIAB trials resulting in lower final disease levels (Table 2). At both locations four disease assessments were recorded seven-eight days apart in the period from 22 June to 14 July 2021. The individual lines showed different phenotypes recorded on the third assessment of the AU trials (Fig. 1). As expected, the Avocet S susceptible control recorded some of the highest disease severity in the experiments, reaching a final 100 percent disease severity in the AU trials (Fig. 2) and 13–19 percent in the NIAB trials (Fig. 3), showing a much slower disease progression under the NIAB conditions. The AUDPC values in AU trials ranged from 103.29 recorded for *Yr18* line infected with Warrior (–) to 1,559.02 for the *PstS2*-infected Avocet S (Table 2). Since the pairs of lines do not have the same genetic background, it only made sense to compare values of the lines within pairs. AUDPC was always lower for the resistant line compared to the susceptible control line in both the AU and NIAB trials, except for the *Yr29* line against the Warrior race in the NIAB trial. The differences were statistically significant under the high disease pressure in the AU trials but in most cases not significant in the NIAB trials. In the AU trial *Yr18* and *Yr46* caused more than 75% reduction of AUDPC values over their susceptible siblings when infected with either pathogen races. Under the lower disease pressure at NIAB, the *Yr18* and *Yr46* caused more than 75% reduction against the Warrior race and more than 50% reduction against the Warrior (–) race. The reduction in AUDPC was less apparent for *Yr29* against all three pathogen races across the two trials, although a 65% reduction was observed against the Warrior (–) race in the AU trial.

The final disease score on the resistant line was always lower than the susceptible line in all trials

without exceptions, and in most cases the difference was statistically significant (Table 2). Again, the strongest effects were observed for *Yr18* and *Yr46* across trials, and *Yr18* was the most effective gene under the high disease pressure. Under the lower disease pressure *Yr18* and *Yr46* appeared a little less effective on final disease score against the Warrior (–) race than against the Warrior race. Highest final disease scores were recorded for *Yr29* under high disease pressure with a final score of 83 percent against the *PstS2* race and 35 percent against the Warrior (–) race, again indicating a lower effect of this gene. In general, the effect of the genes was increasingly apparent with each consecutive scoring (Figs. 2 and 3).

Thousand grain weight

Mean TGW values only recorded in the AU trials were always higher for the Warrior (–) inoculated trial compared to the *PstS2* trial. Furthermore, TGW was always higher in the lines harboring resistance genes when compared to their susceptible siblings but not always statistically significant (Table 2). The TGW values of disease-free control plants grown under greenhouse conditions were much higher than field values (Table 2). In all cases control values were statistically different between sibling lines. For *Yr18* and *Yr46*, however, values recorded on the susceptible line in the greenhouse were higher compared to the line with the APR gene. For *Yr29* the resistant line had higher control values but the difference to the susceptible line was much lower compared to the difference observed in the field.

Fungal biomass quantification

The level of fungal biomass was measured as relative fluorescent units (RFU) on a spectrophotometer after staining fungal structures with the fluorescent dye WGA-FITC. On both dates RFU was always lower in the resistant line against both pathogen races, but the differences were not always statistically significant (Fig. 4). As for AUDPC and final disease score, the greatest reductions in fungal biomass were found on the *Yr18* and *Yr46* resistant lines. Opposite to disease severity, differences were more apparent at the early assessment date.

Table 2 Disease severity indicators (AUDPC and final disease score) and thousand grain weight measurements. Statistical significance levels show the difference between the resistant wheat line and the corresponding susceptible control line within parameters and trials

Line	AUDPC ^a				Final disease score (%) ^b				TGW (g) ^c				
	AU trials		NIAB trials		AU trials		NIAB trials		AU trials		AU trials		Control
	PstS2	Warrior (-)	Warrior (-)	Warrior (-)	PstS2	Warrior (-)	Warrior (-)	Warrior (-)	PstS2	Warrior (-)	Warrior (-)		
Yr18	133 ^{****}	128 [*]	9 ^{ns}	66 ^{ns}	8.8 ^{****}	8.8 ^{****}	0.5 [*]	3.7 [*]	39.1 ^{ns}	39.9 ^{ns}	57.9 ^{**}		
Control (Yr18-)	1435	912	28	124	100	100	4.3	10	34.4	36.3	61.5		
Yr29	1055 ^{****}	446 ^{**}	64 ^{ns}	113 ^{ns}	83.3 ^{ns}	35 [*]	3 [*]	5.7 ^{ns}	32.0 ^{**}	35.2 ^{**}	56.6 [*]		
Control (Yr29-)	1660	1288	54	118	100	75	8	10.7	26.5	27.7	54.3		
Yr46	374 ^{****}	234 [*]	21 ^{**}	104 ^{ns}	29.2 ^{**}	17.5 ^d	1 ^{**}	5.7 ^{ns}	28.5 ^{**}	29.8 [*]	37.8 [*]		
Control (Yr46-)	1821	1570	182	227	100	100	12.3	17.7	23.2	26.9	38.5		
Avocet S	1834	1698	143	230	100	100	13	19	30.1	30.2	No data		

^aArea under disease progress curve calculated from means of four disease severity assessments seven to eight days apart

^bFinal disease scores as percentage leaf area covered by disease assessed on the upper three leaf. Final disease scores were assessed 14 July 2021 at both NIAB and AU

^cThousand grain weight (mean values of three repetitions), including disease-free control plants grown in the greenhouse

* = $P < 0.05$, ** = $P < 0.01$, *** = $P < 0.001$, **** = $P < 0.0001$, ns = $P > 0.05$

^dCould not be compared with t-test due to lack of variation between scorings

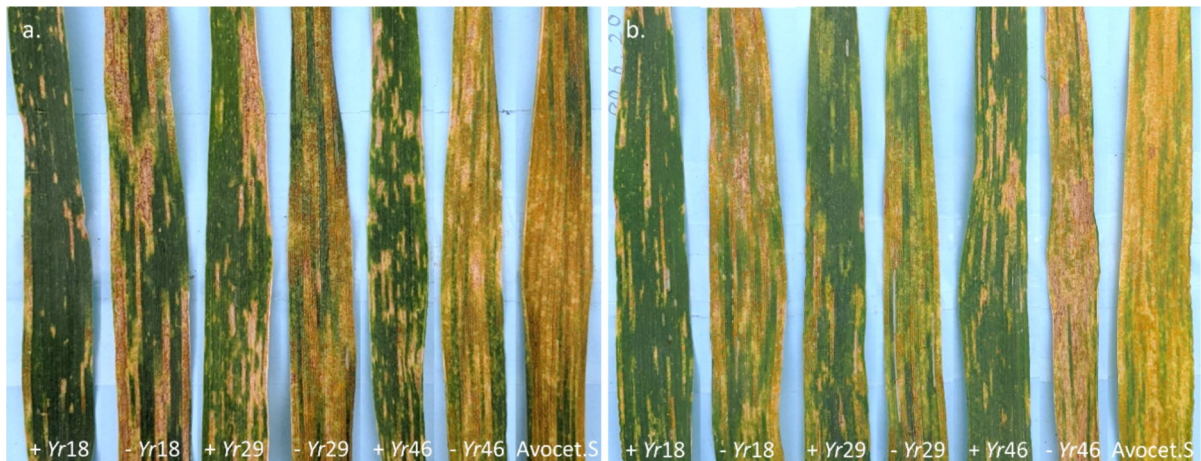


Fig. 1 Example of flag leaf responses of the six experimental spring wheat lines exposed to two different races of wheat yellow rust in the AU field trial at the second assessment date (30 June 2021) **a** *PstS2* (aggressive race), **b** *PstS10/Warrior* (-)

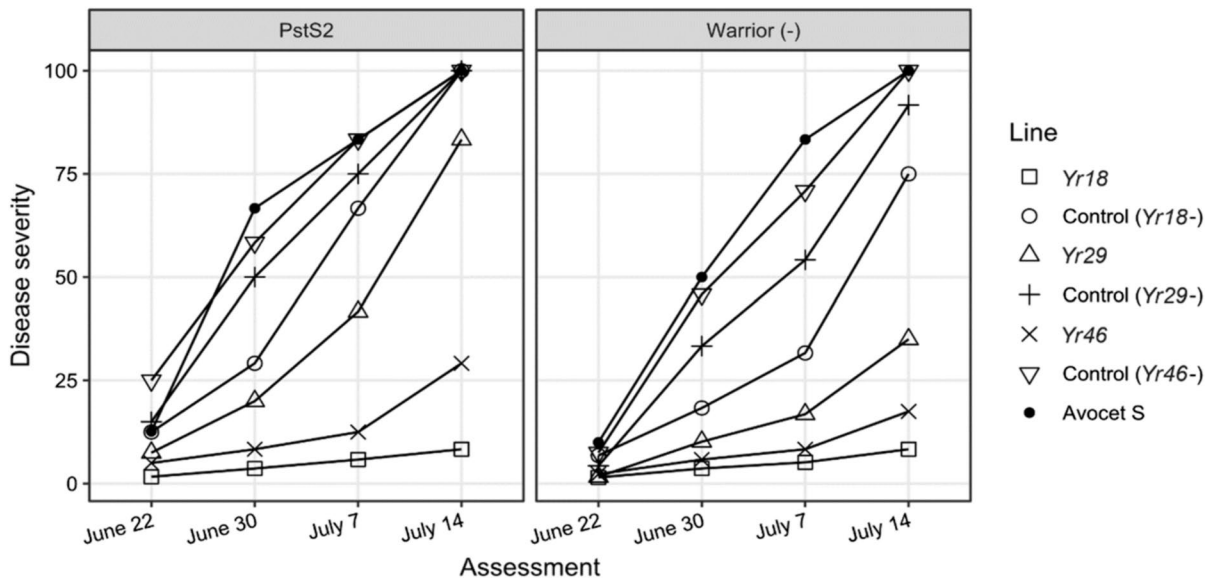


Fig. 2 Disease progress curves for *PstS2* and *Warrior* (-) trials conducted at Aarhus University, Denmark. Disease severity was assessed on the four dates 22 June, 30 June, 7 July and 14 July 2021 using the modified Cobb Scale

Microscopic phenotyping

Stitching fluorescent microscopy photos from the *PstS2* trial yielded images with a size of approximately $26,000 \times 7000$ pixels. Representative images for each wheat line are shown in Fig. 5. The total amount of fungal infection in the images was determined with a threshold function and was up to 39.93%

of the leaf area. In six images the area of fungal infection was below 1% and in those cases the images were not analysed with the U-Net model to estimate the area of uredinia (Fig. 6). They were only checked visually and evaluated with zero as no uredinia were found. In the rest of the images, the model predicted areas with sporulating uredinia, which covered as much as 13.56% of the area. Results show that means

Fig. 3 Disease progress curves for *PstS10* and *PstS7* trials at NIAB, Cambridge. Disease severity was assessed on the four dates 23 June, 30 June, 6 July and 14 July 2021 using the modified Cobb Scale

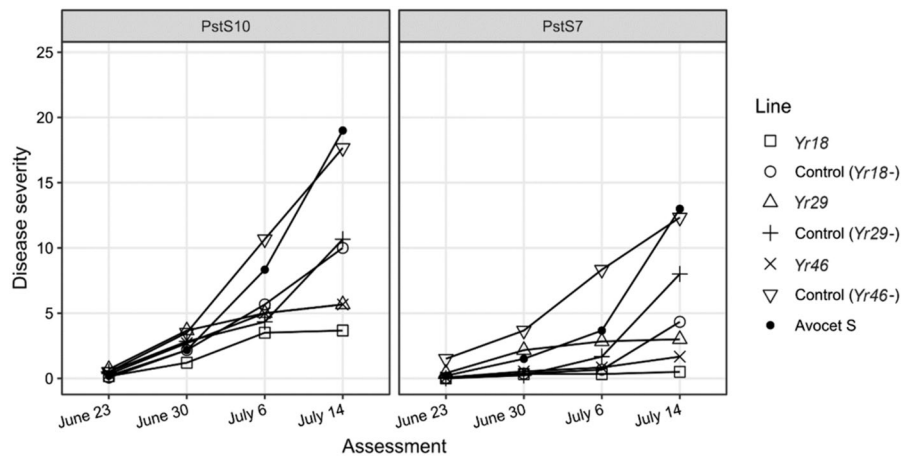
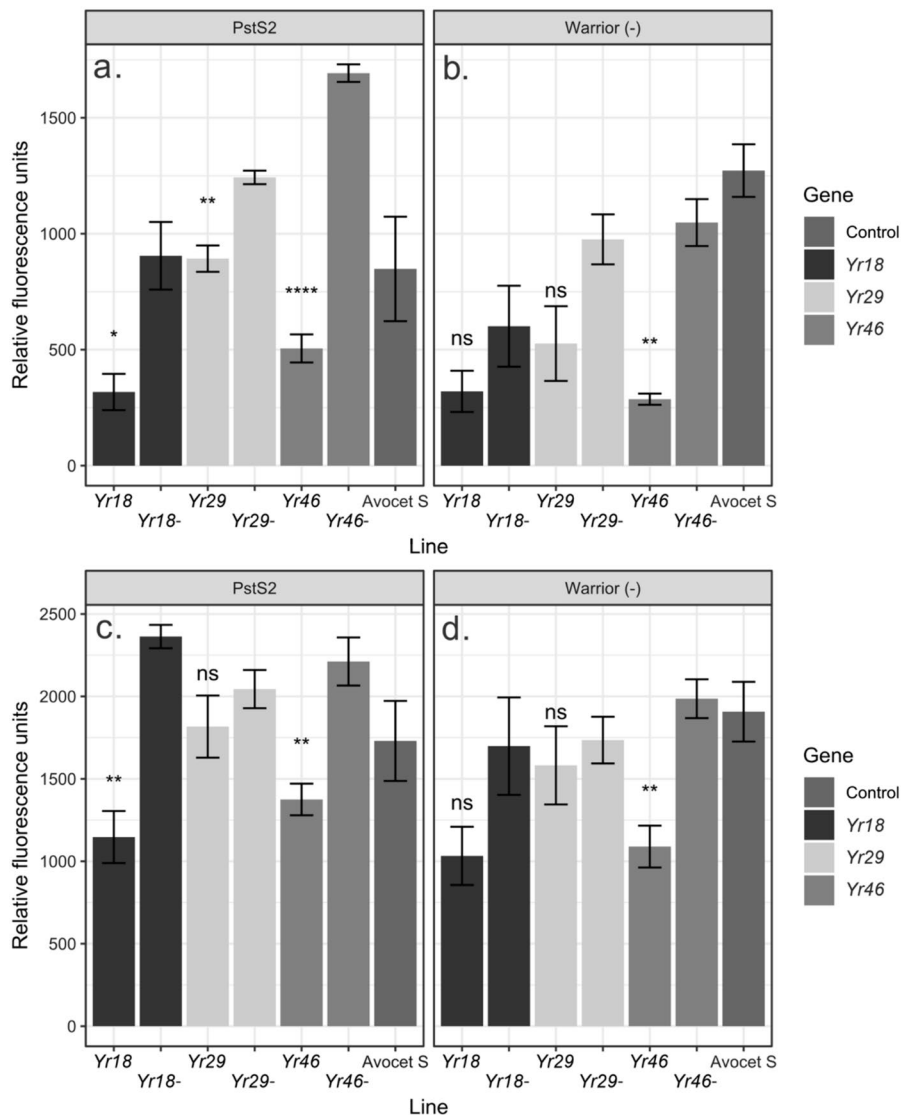


Fig. 4 Fungal tissue in bulked flag leaves were quantified by staining tissue with WGA-FITC followed by measurement of relative fluorescence units. Measurements were done on experimental wheat lines exposed to the Warrior (-) and *PstS2* yellow rust races. Relative fungal tissue levels in samples collected 22 June 2021 in the AU *PstS2* (a) and Warrior (-) (b) field trials. Relative fungal tissue levels in samples collected 7 July 2021 in the AU *PstS2* (c) and Warrior (-) (d) field trials. Error bars represent standard error of the means. * = $P < 0.05$, ** = $P < 0.01$, *** = $P < 0.001$, **** = $P < 0.0001$, ns = $P > 0.05$



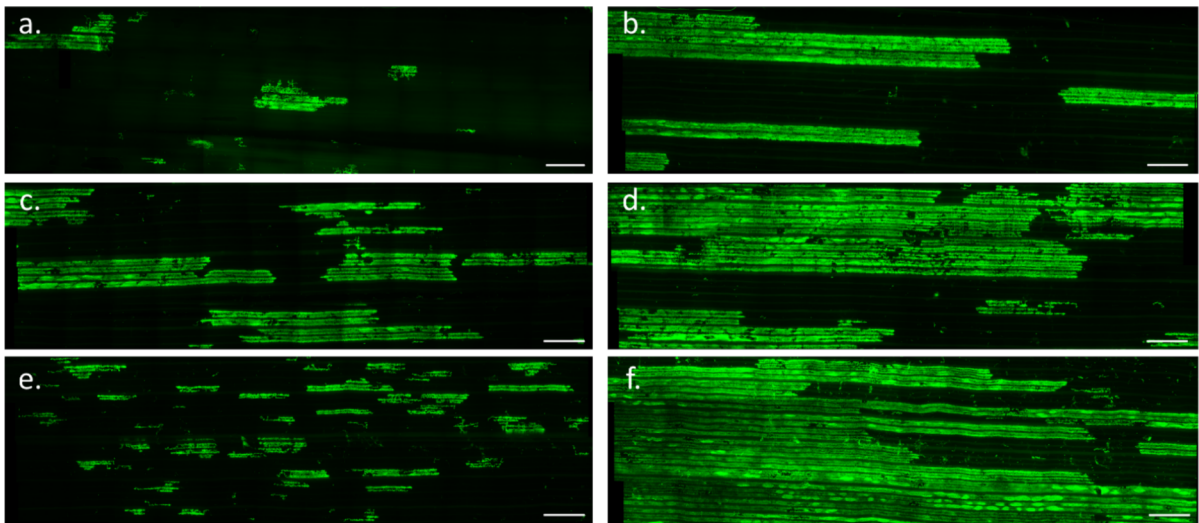
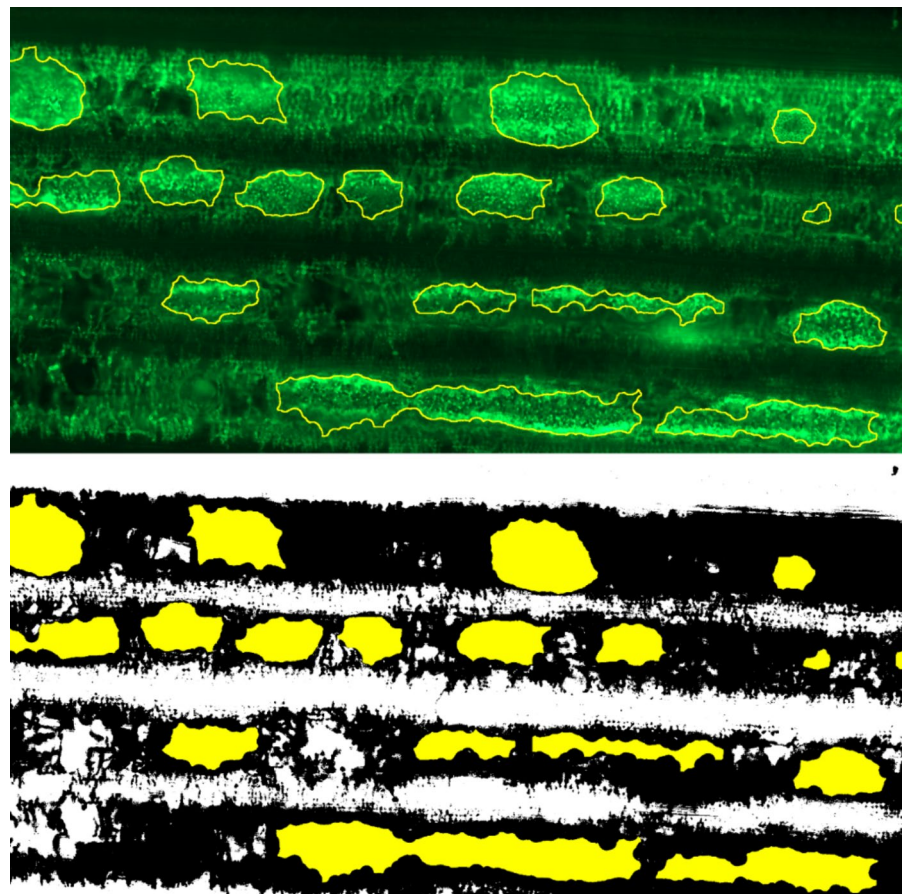


Fig. 5 Representative stitched microscopy images showing the level of fungal infection (green) in leaves of the experimental pairs of sibling lines with or without individual APR genes. Each image is stitched from 48 images in a 12×4 matrix

(length \times width). **a** Sibling line with *Yr18*, **b** Susceptible sibling line without *Yr18*, **c** Sibling line with *Yr29*, **d** Susceptible sibling line without *Yr29*, **e** Sibling line with *Yr46*, **f** Susceptible sibling line without *Yr46*. Scale bars = 2000 μm

Fig. 6 Our newly trained U-Net model predicts uredinia as the sporulating areas of the mycelium. This figure demonstrates the model's prediction on a small area of the leaf as a mask outline on the original microscopy image (top) and as a yellow mask on a black mask that shows total mycelium in the plant leaf (bottom). Areas of the masks were used for quantification of infected and sporulating areas



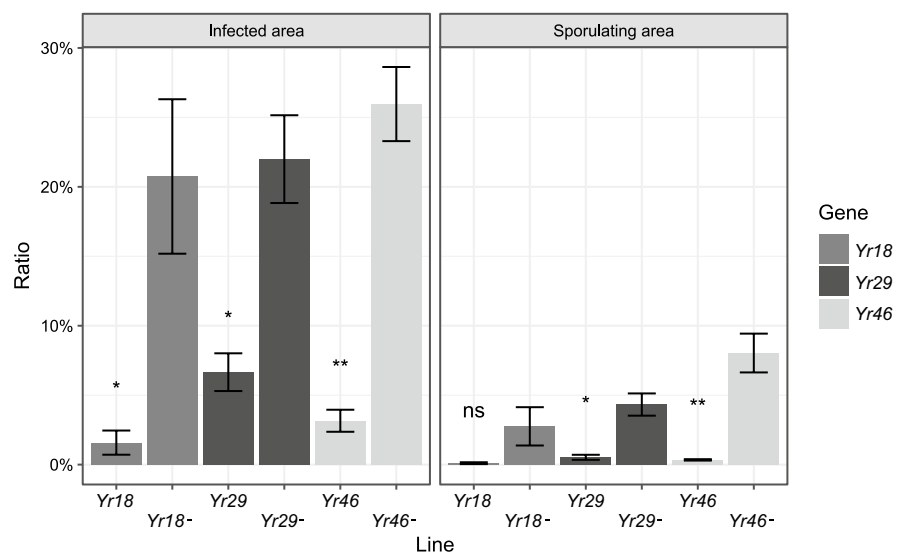
of total infected area were significantly lower on the line with the APR gene and sporulating areas were also reduced although not significantly on the *Yr18* line (Fig. 7). Thus, image analysis confirms the effect the APR genes in slowing down the disease progress in the early stages of development. As for other parameters, the strongest reduction was observed on lines with either the *Yr18* or *Yr46* resistance gene.

Discussion

Field trials in our study were inoculated separately with *Pst* races from three distinct genetic lineages, all with very recent importance in the pathogen's epidemiology. The Warrior (–) race of the genetic group *PstS10* were repeated in the Danish and the UK trials. The *PstS2* race only used in the Danish trials belongs to the genetic group *PstS2* that emerged around 2000 and spread around several continents in the following years causing significant epidemics (Ali et al. 2017). The speed of this spread was facilitated by its increased aggressiveness and adaptation to warmer ecological conditions (Hovmøller et al. 2008; Milus et al. 2009). Indeed, our results also showed that the severity of disease in artificially inoculated wheat was always higher for this very aggressive isolate compared to Warrior (–) (*PstS10*). It is worth noting that our disease trials were undertaken in Northern Europe, and *PstS2* never became dominant in the European continent like it did in West

Asia and North Africa and partly East Africa, probably because of effective resistance genes in European cultivars (Hovmøller et al. 2008). As the two races are compared here, we can also see that *PstS2* would potentially cause more severe decrease in TGW in the field. Although this indicator varies substantially between the individual lines, the mean TGW loss in *PstS2*-inoculated plants was > 5% higher compared to those inoculated with Warrior (–). The Warrior race only used in the UK trials belongs to the *PstS7* strain which emerged in Europe in 2011 and became dominant in the following years. Since then, the Warrior (–) races have taken over and are now the most prevalent races in Europe. In the NIAB trials higher disease levels were generally recorded in the Warrior (–) trial which could indicate that this race is more aggressive or better adapted to the North-West European environment. However, in our experimental design individual trials were carried out for each pathogen race and therefore race comparisons should be done with caution. It is, however, important to test APR genes against distinct pathogen races because even though such genes are usually considered non-race specific, they may in fact be overcome by newly emergent rust strains, and as indicated here, the effect may also depend on pathogen aggressiveness. Race-specificity of APR was previously demonstrated in *Pst*-wheat (Sørensen et al. 2014) and *Puccinia hordei*-barley pathosystems (Marcel et al. 2008). Our results show that *Yr18* and *Yr46* have a good effect against all three races used across trials, whereas *Yr29* in general

Fig. 7 Infected and sporulating areas in microscopy images quantified by image analysis. Samples from *PstS2* field trial, collected during the first disease assessment (June 22). Bars represent mean values, error bars represent standard error of the means. * = $P < 0.05$, ** = $P < 0.01$, ns = $P > 0.05$



was less effective. Trials for testing APR in CIM-MYT spring wheats are usually conducted in Mexico, Ecuador, or Kenya (Singh et al. 2011). Here we show that the effect of individual APR genes *Yr18*, *Yr29* and *Yr46* is also apparent in North-West European conditions, in both an environment where susceptible checks reached maximum disease severity (AU trials), and in an environment with a slower disease progression (NIAB trials). The difference in disease development were likely due to differences in humidity, precipitation, and/or temperature which has a known influence on yellow rust progression on wheat (Te Beest et al. 2008), although these climatic parameters were not measured in the trials. APR expression is also known to vary in different environments (Miedaner and Juroszek 2021) but our results at the two locations indicate a general effect of these APR genes under Northwest European climate conditions, especially *Yr18* and *Yr46* appear highly useful.

The resistance phenotypes of *Lr34/Yr18/Sr57/Pm38* and *Lr67/Yr46/Sr55/Pm46* in field conditions are visually very similar in the leaf rust-wheat pathosystem, although resistance of *Lr34/Yr18/Sr57/Pm38* alone is generally considered stronger than that of *Lr67/Yr46/Sr55/Pm46* (Spielmeyer et al. 2013; Sivasamy et al. 2014; McCallum and Hiebert 2022). The lower effect of *Yr46* was also seen in our trials where AUDPC and final disease score were higher than for *Yr18* across all trials. Again, comparison should be done with caution since the APR genes were tested in different genetic backgrounds, which may contain additional unknown minor APR genes. The *Lr46/Yr29/Sr58/Pm39* is considered to have a similar, but weaker phenotype compared to *Lr34/Yr18/Sr57/Pm38* (Kolmer 2015), which our results also indicated. The lower effectiveness of *Yr29* was also demonstrated by assessment of fungal biomass, but the stronger effect of *Yr18* compared to *Yr46* was less apparent in this analysis. Relative difference between the resistant and susceptible lines were larger and more significant for biomass assessment on the first sampling date. This inconsistency of WGA results may be attributed to a lower accuracy of the method, especially when used for plants grown outside. The method is not specific to one fungal species, and it is expected that other fungi might be present, especially in the older leaves. In disease-free controls in greenhouse, the susceptible plants recorded higher TGW values in case of *Yr18* and *Yr46*. This may be

due to the fitness penalty of the functioning resistance genes (Singh and Huerta-Espino 1997; Brown and Rant 2013).

Thanks to the cloning of two of the resistance genes, *Lr34/Yr18/Sr57/Pm38* and *Lr67/Yr46/Sr55/Pm46*, we know that the coded proteins are different. *Lr34/Yr18/Sr57/Pm38* encodes an adenosin-triphosphate binding cassette (ABC transporter) (Krattinger et al. 2009) which acts as an abscisic acid transporter (Krattinger et al. 2019). Abscisic acid can trigger many mechanisms in plants including disease resistance and Krattinger et al. (2019) suggests that abscisic acid transported by the *Lr34/Yr18/Sr57/Pm38* protein might in fact trigger the same mechanisms that underpin *Yr46* resistance, since they are so phenotypically similar. *Lr67/Yr46/Sr55/Pm46* encodes a sugar transporting protein that belongs to STP13 class as described in *Arabidopsis* (Moore et al. 2015). It has been reasoned that the resistance allele TaSTP13GR in wheat could confer resistance by the loss of glucose transport ability when compared to the functional glucose-transport allele TaSTP13, as this could mean there are less nutrients available for the fungal growth (Milne et al. 2019). A similar effect was observed in barley with orthologous resistance allele HvSTP13GR which is deficient in glucose transport and confers resistance to *P. hordei* (Skoppek et al. 2022). Microscopic observations of Skoppek et al. (2022) show that the rust development is not slowed down until haustorial mother cells are formed and the transport of nutrients from plant to pathogen is established. Milne et al. (2022) in their most recent study argue that the resistance in TaSTP13GR in wheat is in fact a gain-of-function phenotype rather than a side-effect of the reduced sugar transport ability. Interestingly, the team also points out that the resistance phenotype (together with leaf tip necrosis) cannot be usually observed in greenhouse or cultivation chamber conditions unless the mechanism is induced by applying NaCl to the plants. Therefore, it appears that the resistant reaction is not dependent on the pathogen detection by plant. Our microscopic phenotyping results showed that all three genes strongly reduced early leaf colonisation and pustule formation, but again with a lower effect of *Yr29*.

Phenotyping of adult plant resistance is currently considered a bottleneck in studies of quantitative resistance in crops, and there is a need for more accurate phenotyping methods to complement the

large amounts of genotyping data (Cobb et al. 2013). Development of image analysis methods with the use of artificial intelligence is required for high-throughput, automated phenotyping (Zhao et al. 2019). In this study, we demonstrate a phenotyping method incorporating fluorescent microscopy and image analysis with machine learning. Stitched microscopy images allowed us to cover relatively large portions of leaves and thus provide representative samples. With image analysis, we quantified area of the leaf colonized by the fungus, but also the area of sporulating uredinia. Training a deep learning model enabled automation of the second part of the process and this can be easily upscaled for larger dataset sizes. By measuring growth of fungal colony and its sporulation separately, we can now effectively separate individual components of resistance. Sporulation intensity is one of the monocyclic disease processes that influence the resulting epidemics in the field, and epidemiological models calculate with relative resistance to sporulation intensity (RRSP) as one of the components of resistance (Willoquet et al. 2017). Using deep learning to quantify this component of resistance provides high level of automation and will hopefully inspire more future analysis.

Since APR genes are recommended to be combined or stacked with other genes to achieve sufficient resistance, it is appropriate to study their interactions. For example, McCallum and Hiebert (2022) demonstrated that *Lr67/Yr46/Sr55/Pm46* specifically does not increase leaf rust resistance of *Lr13* like *Lr34/Yr18/Sr57/Pm38* does. On the other hand, both genes substantially increase leaf rust resistance of *Lr16* which is insufficient on its own. Cultivars with *Lr67/Yr46/Sr55/Pm46* or a combination of *Lr34/Yr18/Sr57/Pm38* and *Lr46/Yr29/Sr58/Pm39* showed a range of responses in CIMMYT disease trials (Huerta-Espino et al. 2020) where further resistance alleles affected the results. It is therefore necessary to evaluate the genes further in genetic backgrounds where they are to be adopted. It is also worth noting that while the genes have a pleiotropic effect, the strength of their resistance may differ against the individual diseases. When tested against all three wheat rusts in CIMMYT trials, some cultivars with these APR genes performed better against leaf rust and yellow rust but were still moderately susceptible to stem rust (Huerta-Espino et al. 2020) and similar results were shown for *Lr46/Yr29/Sr58/Pm39* specifically

(Kolmer et al. 2015), therefore more minor effect genes might have to be used to control stem rust than the other diseases.

Our experiments demonstrate the individual effect of the three APR genes *Yr18*, *Yr29* and *Yr46* in spring wheat against yellow rust under North-West European field conditions. Lines containing these genes were tested against yellow rust races that have been recently causing damage on wheat. The disease resistance was observed and quantified in artificial inoculation field trials and results indicate that *Yr18*, *Yr29*, and *Yr46* can be recommended for breeding for North-West European conditions, ideally to be stacked with other resistance genes.

Acknowledgements We want to thank gardener Jakob Sørensen for seed multiplication of all experimental lines in the greenhouse, and laboratory technician Ellen Frederiksen for maintenance and multiplication of pathogen isolates.

Author contributions The study was designed and conceived by CKS, PS, SW and OZ. The field experiments and sampling at Aarhus university were done by CKS. Field experiments and sampling at NIAB were performed by SW, AH and CFN. Plant materials were developed and provided by JHE and RS. Biomass analysis was performed by OZ. Microscopy and image analysis was done by OZ, CKS and AKM. Training of AI-model for image analysis was done by OZ. OZ wrote the first draft of the manuscript with contributions from CKS, and all authors gave comments and approved the final manuscript.

Funding Open access funding provided by Aarhus Universitet. The research was funded by the European Commission, Research and Innovation, Horizon 2020-Sustainable Food Security (Grant Number: 773311-2, RustWatch), the Independent research Fund Denmark (Grant Number: 1127-00314B, Tempres) and the Erasmus plus training program, European Union.

Data availability The datasets generated during and/or analysed during the current study are available from the corresponding author on reasonable request.

Declarations

Conflict of interest The authors have no relevant financial or non-financial interests to disclose.

Open Access This article is licensed under a Creative Commons Attribution 4.0 International License, which permits use, sharing, adaptation, distribution and reproduction in any medium or format, as long as you give appropriate credit to the original author(s) and the source, provide a link to the Creative Commons licence, and indicate if changes were made. The images or other third party material in this article are included in the article's Creative Commons licence, unless indicated otherwise in a credit line to the material. If material is not

included in the article's Creative Commons licence and your intended use is not permitted by statutory regulation or exceeds the permitted use, you will need to obtain permission directly from the copyright holder. To view a copy of this licence, visit <http://creativecommons.org/licenses/by/4.0/>.

References

- Ali S, Rodriguez-Algaba J, Thach T, Sørensen CK, Hansen JG, Lassen P, Nazari K, Hodson DP, Justesen AF, Hovmøller MS (2017) Yellow rust epidemics worldwide were caused by pathogen races from divergent genetic lineages. *Front Plant Sci* 8:1057. <https://doi.org/10.3389/fpls.2017.01057>
- Ayliffe M, Periyannan SK, Feechan A, Dry I, Schumann U, Wang M-B, Pryor A, Lagudah E (2013) A simple method for comparing fungal biomass in infected plant tissues. *Mol Plant Microbe Interact* 26:658–667. <https://doi.org/10.1094/MPMI-12-12-0291-R>
- Beddow JM, Pardey PG, Chai Y, Hurley TM, Kriticos DJ, Braun HJ, Park RF, Cuddy WS, Yonow T (2015) Research investment implications of shifts in the global geography of wheat stripe rust. *Nat Plants*. <https://doi.org/10.1038/nplants.2015.132>
- Brown JK, Rant JC (2013) Fitness costs and trade-offs of disease resistance and their consequences for breeding arable crops. *Plant Pathol* 62:83–95. <https://doi.org/10.1111/ppa.12163>
- Cobb JN, DeClerck G, Greenberg A, Clark R, McCouch S (2013) Next-generation phenotyping: requirements and strategies for enhancing our understanding of genotype–phenotype relationships and its relevance to crop improvement. *Theor Appl Genet* 126:867–887. <https://doi.org/10.1007/S00122-013-2066-0>
- Ellis JG, Lagudah ES, Spielmeier W, Dodds PN (2014) The past, present and future of breeding rust resistant wheat. *Front Plant Sci* 5:641. <https://doi.org/10.3389/fpls.2014.00641>
- Falk T et al (2018) U-Net: deep learning for cell counting, detection, and morphometry. *Nat Methods* 16:67–70. <https://doi.org/10.1038/s41592-018-0261-2>
- Hovmøller MS, Yahyaoui AH, Milus EA, Justesen AF (2008) Rapid global spread of two aggressive strains of a wheat rust fungus. *Mol Ecol* 17:3818–3826. <https://doi.org/10.1111/J.1365-294X.2008.03886.X>
- Hovmøller MS, Rodriguez-Algaba J, Thach T, Sørensen CK (2017) Race typing of *Puccinia striiformis* on wheat. *Wheat Rust Dis Methods Protoc*. https://doi.org/10.1007/978-1-4939-7249-4_3
- Hovmøller MS, Patpour M, Rodriguez-Algaba J, Thatch T, Sørensen CK, Justesen AF, Hansen J (2023) GRRC 2022 report of stem and yellow rust genotyping and race analyses. GRRC, Aarhus University, Denmark. https://agro.au.dk/fileadmin/www.grcc.au.dk/International_Services/Pathotype_YR_results/GRRC_annual_report_2022.pdf. Assessed 01 Dec 2023
- Hovmøller MS et al (2016) Replacement of the European wheat yellow rust population by new races from the centre of diversity in the near-Himalayan region. *Plant Pathol* 65:402–411. <https://doi.org/10.1111/ppa.12433>
- Huerta-Espino J, Singh R, Crespo-Herrera LA, Villaseñor-Mir HE, Rodriguez-Garcia MF, Dreisigacker S, Barcenan-Santana D, Lagudah E (2020) Adult plant slow rusting genes confer high levels of resistance to rusts in bread wheat cultivars from Mexico. *Front Plant Sci* 11:1–15. <https://doi.org/10.3389/fpls.2020.00824>
- Kolmer JA (2015) A QTL on chromosome 5BL in wheat enhances leaf rust resistance of *Lr46*. *Mol Breed* 35:1–8. <https://doi.org/10.1007/s11032-015-0274-9>
- Kolmer JA et al (2008) Analysis of the *Lr34/Yr18* rust resistance region in wheat germplasm. *Crop Sci* 48:1841–1852. <https://doi.org/10.2135/cropsci2007.08.0474>
- Kolmer JA, Lagudah ES, Lillemo M, Lin M, Bai G (2015) The *Lr46* gene conditions partial adult-plant resistance to stripe rust, stem rust, and powdery mildew in Thatcher wheat. *Crop Sci* 55:2557–2565. <https://doi.org/10.2135/cropsci2015.02.0082>
- Krattinger SG, Lagudah ES, Spielmeier W, Singh RP, Huerta-Espino J, McFadden H, Bossolini E, Selter LL, Keller B (2009) A putative ABC transporter confers durable resistance to multiple fungal pathogens in wheat. *Science* 323:1360–1363. <https://doi.org/10.1126/science.1166453>
- Krattinger SG et al (2019) Abscisic acid is a substrate of the ABC transporter encoded by the durable wheat disease resistance gene *Lr34*. *New Phytol* 223:853–866. <https://doi.org/10.1111/NPH.15815>
- Lagudah ES (2011) Molecular genetics of race non-specific resistance in wheat. *Euphytica* 179:81–91. <https://doi.org/10.1007/S10681-010-0336-3>
- Legland D, Arganda-Carreras I, Andrey P (2016) MorphoLibJ: integrated library and plugins for mathematical morphology with ImageJ. *Bioinformatics* 32:3532–3534. <https://doi.org/10.1093/BIOINFORMATICS/BTW413>
- Marcel TC, Gorguet B, Ta MT, Kohutova Z, Vels A, Niks RE (2008) Isolate specificity of quantitative trait loci for partial resistance of barley to *Puccinia hordei* confirmed in mapping populations and near-isogenic lines. *New Phytol* 177:743–755. <https://doi.org/10.1111/J.1469-8137.2007.02298.X>
- McCallum BD, Hiebert CW (2022) Interactions between *Lr67* or *Lr34* and other leaf rust resistance genes in wheat (*Triticum aestivum*). *Front Plant Sci*. <https://doi.org/10.3389/fpls.2022.871970>
- Miedaner T, Juroszek P (2021) Climate change will influence disease resistance breeding in wheat in Northwestern Europe. *Theor Appl Genet* 134:1771–1785. <https://doi.org/10.1007/s00122-021-03807-0>
- Milne RJ, Dibley KE, Schnippenkoetter W, Mascher M, Lui ACW, Wang L, Lo C, Ashton AR, Ryan PR, Lagudah ES (2019) The wheat *Lr67* gene from the sugar transport protein 13 family confers multipathogen resistance in barley. *Plant Physiol* 179:1285–1297. <https://doi.org/10.1104/pp.18.00945>
- Milne RJ, Dibley KE, Bose J, Riaz A, Zhang J, Schnippenkoetter W, Ashton AR, Ryan PR, Tyerman SD, Lagudah ES (2022) The wheat multi-pathogen resistance gene, *Lr67res*, confers a novel gain-of-function phenotype

- involving anion fluxes. bioRxiv:2022.03.22.485337. <https://doi.org/10.1101/2022.03.22.485337>
- Milus EA, Kristensen K, Hovmøller MS (2009) Evidence for increased aggressiveness in a recent widespread strain of *Puccinia striiformis* f. sp. *tritici* causing stripe rust of wheat. *Phytopathology* 99:89–94. <https://doi.org/10.1094/PHYTO-99-1-0089>
- Moore JW et al (2015) A recently evolved hexose transporter variant confers resistance to multiple pathogens in wheat. *Nat Genet* 47:1494–1498. <https://doi.org/10.1038/ng.3439>
- Peterson RF, Campbell AB, Hannah AE (1948) A diagrammatic scale for estimating rust intensity on leaves and stems of cereals. *Can J Res* 26c:496–500. <https://doi.org/10.1139/cjr48c-033>
- R Core Team (2021) A Language and environment for statistical computing. R foundation for statistical computing, Vienna, Austria. <https://www.R-project.org/>
- Roelfs AP, Singh RP, Saari EE (1992) Rust diseases of wheat: concepts and methods of disease management. CIMMYT, Mexico
- Schindelin J et al (2012) Fiji: an open-source platform for biological-image analysis. *Nat Methods* 9:676–682. <https://doi.org/10.1038/nmeth.2019>
- Singh R, Huerta-Espino J (1997) Effect of leaf rust resistance gene *Lr34* on grain yield and agronomic traits of spring wheat. *Crop Sci* 37:390–395. <https://doi.org/10.2135/cropsci1997.0011183X003700020014x>
- Singh RP, Mujeeb-Kazi A, Huerta-Espino J (1998) *Lr46*: a gene conferring slow-rusting resistance to leaf rust in wheat. *Phytopathology* 88:890–894. <https://doi.org/10.1094/PHYTO.1998.88.9.890>
- Singh RP et al (2011) Race non-specific resistance to rust diseases in CIMMYT spring wheats. *Euphytica* 179:175–186. <https://doi.org/10.1007/s10681-010-0322-9>
- Sivasamy M, Aparna M, Kumar J, Jayaprakash P, Vikas V, John P, Nisha R, Satyaprakash SK, Punniakotti E (2014) Phenotypic and molecular confirmation of durable adult plant leaf rust resistance (APR) genes *Lr34+*, *Lr46+* and *Lr67+* linked to leaf tip necrosis (LTN) in select registered Indian wheat (*T. aestivum*) genetic stocks. *Cereal Res Commun* 42:262–273. <https://doi.org/10.1556/CRC.2013.0054>
- Skoppek CI, Punt W, Heinrichs M, Ordon F, Wehner G, Boch J, Streubel J (2022) The barley *HvSTP13GR* mutant triggers resistance against biotrophic fungi. *Mol Plant Pathol* 23:278–290. <https://doi.org/10.1111/MPP.13161>
- Sørensen CK, Hovmøller MS, Leconte M, Dedryver F, de Vallavieille-Pope C (2014) New races of *Puccinia striiformis* found in Europe reveal race specificity of long-term effective adult plant resistance in wheat. *Phytopathology* 104:1042–1051. <https://doi.org/10.1094/PHYTO-12-13-0337-R>
- Sørensen CK, Thach T, Hovmøller MS (2016) Evaluation of spray and point inoculation methods for the phenotyping of *Puccinia striiformis* on wheat. *Plant Dis* 100:1064–1070. <https://doi.org/10.1094/PDIS-12-15-1477-RE>
- Spielmeier W, Mago R, Wellings C, Ayliffe M (2013) *Lr67* and *Lr34* rust resistance genes have much in common - they confer broad spectrum resistance to multiple pathogens in wheat. *BMC Plant Biol* 13:1–9. <https://doi.org/10.1186/1471-2229-13-96>
- Te Beest DE, Paveley ND, Shaw MW, van den Bosch F (2008) Disease-weather relationships for powdery mildew and yellow rust on winter wheat. *Phytopathology* 98:609–617. <https://doi.org/10.1094/PHYTO-98-5-0609>
- von Chamier L et al (2021) Democratizing deep learning for microscopy with ZeroCostDL4Mic. *Nat Commun* 12:1–18. <https://doi.org/10.1038/s41467-021-22518-0>
- Wang M, Chen X (2017) Stripe rust resistance. *Stripe Rust*. https://doi.org/10.1007/978-94-024-1111-9_5
- Wellings CR, Singh RP, Yahyaoui A, Nazari K, McIntosh RA (2009). The development and application of near-isogenic lines for monitoring cereal rust pathogens. In: McIntosh RA (ed) Proc Borlaug global rust initiative technical workshop. BGRI Cd Obregon, Mexico, pp 77–87
- Wickham H (2009) Ggplot2: elegant graphics for data analysis, 1st edn. <https://doi.org/10.1007/978-0-387-98141-3>
- Wilcoxon RD, Skovmand B, Atif AH (1975) Evaluation of wheat cultivars for ability to retard development of stem rust. *Ann Appl Biol* 80:275–281. <https://doi.org/10.1111/J.1744-7348.1975.TB01633.X>
- Willocquet L, Savary S, Yuen J (2017) Multiscale phenotyping and decision strategies in breeding for resistance. *Trends Plant Sci* 22:420–432. <https://doi.org/10.1016/j.tplants.2017.01.009>
- Zadoks JC, Chang TT, Konzak CF (1974) A decimal growth code for the growth stages of cereals. *Weed Res* 14:415–421
- Zhao C, Zhang Y, Du J, Guo X, Wen W, Gu S, Wang J, Fan J (2019) Crop phenomics: current status and perspectives. *Front Plant Sci* 10:433490. <https://doi.org/10.3389/fpls.2019.00714>

Publisher's Note Springer Nature remains neutral with regard to jurisdictional claims in published maps and institutional affiliations.